Journal of Maps

ISSN: (Print) (Online) Journal homepage: www.tandfonline.com/journals/tjom20

Late Pleistocene to Holocene glacial, periglacial, and paraglacial geomorphology of the upper Río Limarí basin (30–31° S) in the Andes of central Chile

Javiera Carraha, Juan-Luis García, Samuel U. Nussbaumer, Hans Fernández-Navarro & Isabelle Gärtner-Roer

To cite this article: Javiera Carraha, Juan-Luis García, Samuel U. Nussbaumer, Hans Fernández-Navarro & Isabelle Gärtner-Roer (2024) Late Pleistocene to Holocene glacial, periglacial, and paraglacial geomorphology of the upper Río Limarí basin (30–31° S) in the Andes of central Chile, Journal of Maps, 20:1, 2329179, DOI: 10.1080/17445647.2024.2329179

To link to this article: https://doi.org/10.1080/17445647.2024.2329179

© 2024 The Author(s). Published by Informa UK Limited, trading as Taylor & Francis Group on behalf of Journal of Maps

View supplementary material

Published online: 12 Apr 2024.

Submit your article to this journal

Article views: 479

View related articles

View Crossmark data

Full Terms & Conditions of access and use can be found at
https://www.tandfonline.com/action/journalInformation?journalCode=tjom20

JOURNAL OF MAPS
2024, VOL. 20, NO. 1, 2329179
https://doi.org/10.1080/17445647.2024.2329179

Taylor & Francis
Taylor & Francis Group

Science

OPEN ACCESS Check for updates

Late Pleistocene to Holocene glacial, periglacial, and paraglacial geomorphology of the upper Río Limarí basin (30–31° S) in the Andes of central Chile

Javiera Carraha[a,b], Juan-Luis García[a,b], Samuel U. Nussbaumer[c], Hans Fernández-Navarro[d] and Isabelle Gärtner-Roer[c]

[a]Instituto de Geografía, Facultad de Historia, Geografía y Ciencia Política, Pontificia Universidad Católica de Chile, Santiago, Chile; [b]Centro UC Desierto de Atacama, Pontificia Universidad Católica de Chile, Santiago, Chile; [c]Department of Geography, University of Zurich, Zurich, Switzerland; [d]Instituto de Ciencias Agroalimentarias, Animales y Ambientales (ICA3), Universidad de O'Higgins, San Fernando, Chile

ABSTRACT

We present a field-based reconstruction of the geomorphology in the Subtropical Andean mountains of the Limarí basin, semiarid central Chile (30–31° S). Fieldwork campaigns and remote-sensing analysis served for detailed geomorphological mapping at four formerly glaciated valleys in the heads of the Combarbalá and Río Hurtado sub-basins. We identify a mosaic of glacial, periglacial, and paraglacial landforms. Glacial landforms include a massive dead-ice moraine complex, with thermokarst and debris-filled fractures suggesting former ice-cored moraine degradation. This landform is superimposed by transversal and arcuate ridges suggesting active-ice processes. Periglacial landforms such as rock glaciers, gelifluction, and protalus lobes occur in cirques and U-shaped valleys, but also on moraine deposits. Paraglacial processes are indicated by talus accumulation in those formerly glaciated slopes. The geomorphological imprint is evidence for the interaction and succession between glacial, periglacial, and paraglacial dynamics from the Late Pleistocene to the present.

ARTICLE HISTORY
Received 31 March 2023
Revised 20 November 2023
Accepted 5 March 2024

KEYWORDS
Geomorphology; cryosphere; Glacial, paraglacial and periglacial landforms; geomorphological mapping; Subtropical Andes

1. Introduction

Mountain geomorphology is key for understanding atmosphere-cryosphere interactions in link to climate changes (Fernández-Navarro et al., 2023; García et al., 2014; Knight & Harrison, 2014; Lira et al., 2022; Mackintosh et al., 2017). As glaciers advance and retreat, they erode, transport, and deposit sediments, building landforms as valuable geomorphological evidence to be used in the reconstruction of past regional climate (Anderson et al., 2014; Zech et al., 2008). Moreover, climate changes trigger complex transformations of the mountain cryosphere resulting in distinct geomorphic arrangements related to glacial, periglacial, and paraglacial processes and deposits (Ballantyne, 2002; Benn & Owen, 2002; Fernández et al., 2022; Haeberli & Beniston, 1998). Thus, abundant cryo-geomorphic landforms in high mountains represent valuable archives that can be interpreted for past environmental changes and used as a base for future climate-mountain scenarios (Benn & Owen, 2002). However, the origin and processes of mountain landforms as well as the evolution of the cryosphere in the Subtropical Andes remains mostly unresolved.

The Andes of central Chile (30–35° S) is a conspicuous mountain region where landforms originating from the last glacial period are widespread and well-preserved in multiple valleys (Caviedes & Paskoff, 1975; Charrier et al., 2019; Fernández et al., 2022; García et al., 2014; Paskoff, 1977; Santana, 1967; Zech et al., 2017). Studies have focused on the deglaciation of the Andean glaciers in response to warm and dry periods (e.g. Fernández et al., 2022; García et al., 2014; Janke et al., 2015). Current negative glacier mass balance leads to debris-covered and stagnant glacier snouts, which could evolve to ice-cored moraines, and eventually to dead-ice moraines when the ice finally has melted (Fernández et al., 2022; García et al., 2014). Therefore, the valley bottoms are characterized by a hummocky terrain originated by the *in situ* degradation of inactive debris-rich ice. Other studies have argued that the transition from bare-ice glaciers to debris-covered glaciers may end up developing rock glaciers in response to a warming/drying climate (Anderson et al., 2018; Janke et al., 2015).

Rock glaciers are features characteristic of periglacial settings and permafrost conditions (e.g. Barsch,

CONTACT Javiera Carraha jpcarraha@uc.cl Facultad de Historia, Geografía y Ciencia Política, Instituto de Geografía, Pontificia Universidad Católica de Chile, Av. Vicuña Mackenna 4860, Macul, Santiago, Chile
Supplemental data for this article can be accessed online at https://doi.org/10.1080/17445647.2024.2329179.

© 2024 The Author(s). Published by Informa UK Limited, trading as Taylor & Francis Group on behalf of Journal of Maps
This is an Open Access article distributed under the terms of the Creative Commons Attribution-NonCommercial License (http://creativecommons.org/licenses/by-nc/4.0/), which permits unrestricted non-commercial use, distribution, and reproduction in any medium, provided the original work is properly cited. The terms on which this article has been published allow the posting of the Accepted Manuscript in a repository by the author(s) or with their consent.

1996; Capps, 1910; Wahrhaftig & Cox, 1959), although their genesis and variety is debated. The controversy regarding the origin and dynamics of rock glaciers in the Andes of central Chile has been addressed by different authors (e.g. Azócar & Brenning, 2010; Brenning, 2005; Brenning & Trombotto, 2006; Ferrando & Sarricolea, 2020; Janke et al., 2015; Monnier et al., 2014; Monnier & Kinnard, 2012, 2015, 2017) acknowledging that these landforms are key to understand the mechanisms of the mountain cryosphere and landscape's transition from glacial to paraglacial and periglacial environments (Clark et al., 1998; Giardino & Vitek, 1988; Knight, 2019; Knight et al., 2019; Monnier & Kinnard, 2012).

With this study, we aim to reconstruct the geomorphic imprint of the last glaciation and subsequent deglaciation in the Andean mountains of the Limarí basin (30–31° S), semiarid central Chile. For this, detailed mapping of the glacial, periglacial, and paraglacial geomorphology of several catchments is presented, which denotes mountain environmental progression from past to present, and moreover provides a framework for future geochronological studies.

2. Study area

The mapping area for this study is part of the Andean zone of the Río Limarí basin. The basin, located in the Región de Coquimbo, central Chile, extends approximately from 30°09′ S to 31°22′ S, between the international border with Argentina and the Pacific Ocean. We studied four formerly glaciated valleys where glacial landforms are well-preserved. Although there is no current glacier presence, the cryosphere is represented by widespread rock glaciers and other landforms resulting from periglacial influence. These valleys are located in two sub-basins: Río Hurtado and Río Combarbalá, comprising both the northern and southern ends of the basin, respectively (Figure 1). By including four different valleys we aim to include a more representative geomorphic context for the Andes in this region. In the Río Hurtado sub-basin, the El Viento (30°38′ S) and the El Despoblado (30° 31′ S) valleys were mapped. Elevations range from 3000 m a.s.l. until 5400 m a.s.l. on the highest peaks. In the Río Combarbalá sub-basin, we mapped El Toro (31°17′ S) and Las Arenas (31°20′ S) valleys; elevations range from 2700 m a.s.l. up to 4000 m a.s.l. on the highest peaks, significantly lower than in the Río Hurtado sub-basin. The regional glacier equilibrium-line altitude (ELA) is located at ~5000 m a.s.l. at 27° S, descending to 4500 m a.s.l. at 32° S (Carrasco et al., 2005; Janke et al., 2015). Today, few glaciers are identified in the Río Limarí basin. In contrast, a significant area of the basin, estimated at 25.6 km^2, is occupied by rock glaciers (Azócar & Brenning, 2010; DGA, 2022).

The semiarid Andes of central Chile are in the northern zone of mid-latitude westerly wind influence, south of where the Arid Diagonal intersects the Andes. In this region, precipitation occurs predominately during the austral winter months (Garreaud, 2009). The wintertime weakening of the South Pacific Anticyclone together with the northward expansion of the South Westerly Wind belt allows the storm tracks to bring precipitation to the study area (Garreaud, 2009; May et al., 2011; Quintana & Aceituno, 2012; Sagredo & Lowell, 2012). Precipitation in the Río Limarí basin amounts to 400 mm/yr at 4000 m a.s.l. (Zech et al., 2007). Nonetheless, the El Niño Southern Oscillation (ENSO) has an important influence on the interannual variation regime of precipitation in the Subtropical Andes, making the record highly variable throughout the years (Quintana & Aceituno, 2012). For more than a decade the snow precipitation and thus glaciers of the Andes of central Chile have been affected by a long-term dry spell (the Mega-Drought; Garreaud et al., 2020).

As recorded by Zech et al. (2008, 2017) in Cordón de Doña Rosa (30° S) and El Encierro valley (29° S), successive glacial advances had occurred in this region during the last glacial period, including an extensive advance in Marine Isotope Stage (MIS) 3 and advances in phase with the global Last Glacial Maximum (LGM) between ~26 and 20 ka. Aguilar et al. (2022) confirmed the LGM glacial advances in El Encierro valley and concluded that ice mostly abandoned the main valley by ~18 ka. Based on the available geomorphological and chronological work developed in the region, the timeframe for the landforms described here could date to Late Pleistocene to the Holocene, but ongoing work is expected to provide better temporal constraints for this geomorphic record in the near future.

3. Methods

Maps were produced using a combination of remote-sensing analysis and repeated fieldwork. Remote mapping was carried out using national GEOTEC aerial panchromatic photographs (at a scale of 1:50,000) from the years 1996 and 2000. We produced an ALOS PALSAR DEM (12.5 m spatial resolution) for the delimitation of the valleys and analyzed Google Earth Pro (from the years 2008, 2010, 2019, 2021) and ESRI Base Map images (from the years 2021 and 2022) for mapping. Maps projection and datum is UTM 19S, WGS 84. Fieldwork was carried out in four different campaigns. Río Combarbalá sub-basin was visited in January and November 2020, and Río Hurtado sub-basin was visited in January 2022 and 2023. Observations were documented and georeferenced in draft maps. Identification criteria for landforms used for our mapping are provided in Table 1 and are based on extensive literature revision (e.g. Ballantyne, 2002; Benn & Evans, 2010; Fernández et al., 2022; García et al., 2017;

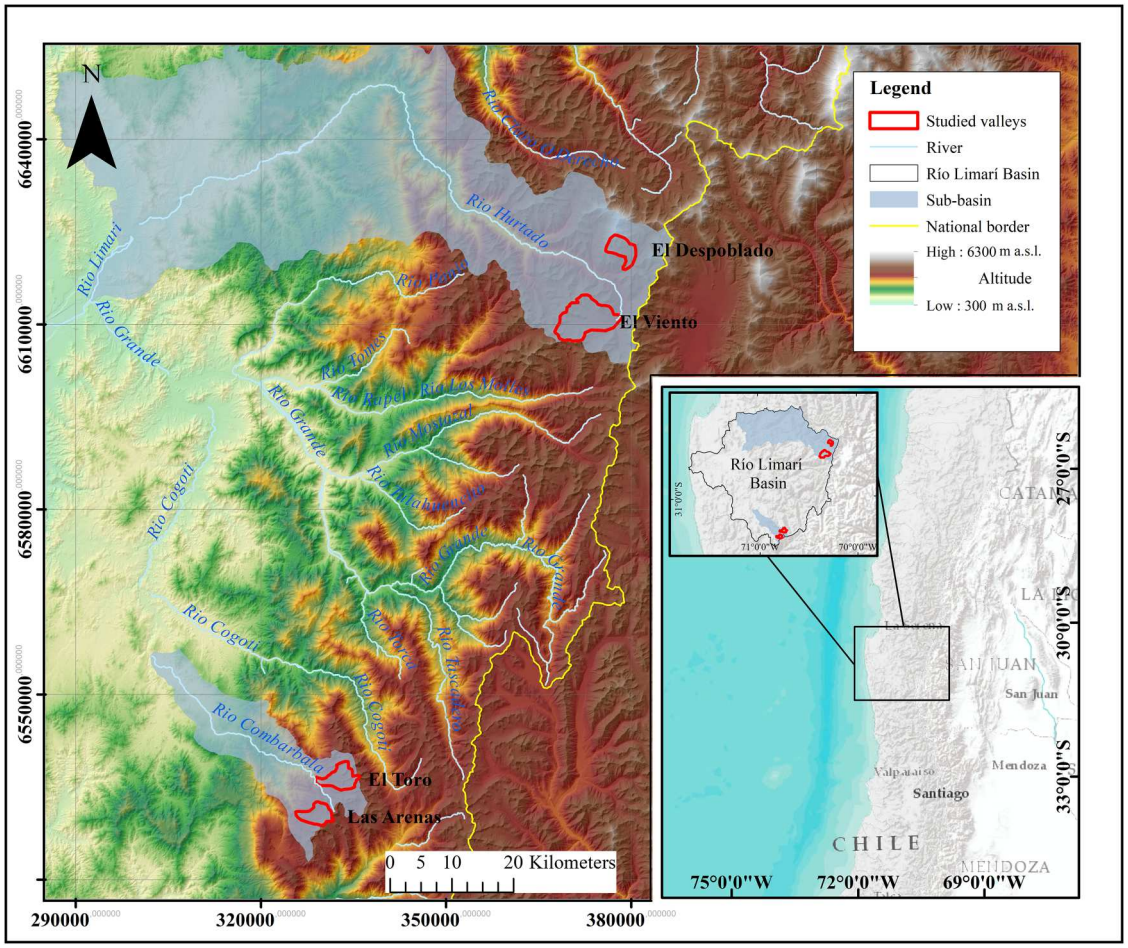

Figure 1. Study area. Digital Elevation Model (ALOS PALSAR and hillshade) of the study area. The red polygons demark the studied valleys. The yellow line represents the Chilean border with Argentina, as obtained from IDE (Infraestructura de Datos Geoespaciales de Chile). Note that the representation of the international limit has been authorized for a scale of 1:50,000, any representation at larger scales may not fully correspond to the drawing of the official limits. Sub-basin and river information was also obtained from IDE. Map scale is 1:750,000 on main map and 1:10,000,000 on the reference map.

Gutiérrez Elorza, 2008). Moraines were analyzed and subdivided into units to establish the generation order in which they were deposited by glaciers. This analysis was made according mostly to the morphostratigraphy but also the lithostratigraphy of these sedimentary sequences. Hughes et al. (2005) use the term morpholithostratigraphy to refer to these types of analysis that are based on the surface form as well as the lithological properties of the deposits (Hughes, 2010).

4. Results

Geomorphological mapping resulted in a mosaic of landforms associated with glacial, periglacial, and paraglacial origins, implying complex setting and sequence of intercalated dominant morphogenetic processes within the studied mountain valleys (see main geomorphic map in Supplementary material).

4.1. Glacial geomorphology

Glacial landforms include those generated by glacial erosion and glacial deposition. From the latter, we separate between landforms determined by active ice processes (i.e. moraine ridges) and inactive ice-derived landforms (i.e. hummocky moraine) *sensu* Fernández et al. (2022).

4.1.1. Glacial erosional landforms

Landforms derived by glacial erosion include large-scale glacial cirques and U-shaped valleys, as well as intermediate-scale landforms such as ice-scoured bedrock (Benn & Evans, 2010; Gordon, 1981; Gutiérrez Elorza, 2008).

4.1.1.1. U-shaped valleys. Cross-sections of valleys are U-shaped. They are delimited by the up-valley headwalls of cirques and the aretes down-valley. These U-shaped valleys are characterized by curved slopes close to the base (15–20°) to steeper slopes in the highest parts (~30°), indicative of glacial erosion. The base of the valleys is relatively flat and wide that progressively narrows down-valley. Most of these valleys are carved along 5–10 km and to the southwest (e.g. Río Combarbalá) or southeast (e.g. Río Hurtado).

Table 1. Identification criteria for the mapping of landforms.

Landform	Description	Reference
Cirque	Amphitheater with abrupt slopes that was or continues to be occupied by ice. Its basal surface is generally smooth.	(Evans & Cox, 1974; Gutiérrez Elorza, 2008)
U-shaped valley	Valley with 'U' shape, with relatively flat bottom and steep slopes.	(Gutiérrez Elorza, 2008)
Ice-scoured bedrock	Extensive development of low rock hills and closed depressions eroded by the action of ice. They commonly occur as roches moutonnées.	(Gordon, 1981)
Moraine	Accumulation of glacial debris marking former glacier extensions.	(Benn & Evans, 2010)
Moraine ridge	Sharp, linear ridges of positive relief that represent the margins of a former glacier. They can form on the sides of glaciers (lateral moraines); on its forehead (terminal/frontal moraine); in the subglacial zone (basal moraine); or in the supraglacial zone (supraglacial moraine). Moraines may be composed of a system of multiple moraine ridges or of a single ridge.	(Anderson & Anderson, 2010; Bendle et al., 2017)
Hummocky terrain	Sedimentary deposits in the form of irregular mounds and depressions with a smooth relief. They can form when supraglacial debris are deposited during periods of differentiated ablation of glacial ice. Mound ridges are less defined than moraine ridges.	(Morén et al., 2011)
Talus rock glacier	Debris body with signs of interstitial ice content formed by detrital accumulations at the base of slopes. It is lobated in shape and presents steep margins. It may contain flow structures.	(Barsch, 1996; Ferrando et al., 2015; García et al., 2017; Gutiérrez Elorza, 2008; Serrano et al., 2011)
Cirque rock glacier	Lobated or tongue-shaped debris body with signs of interstitial ice content located in the cirques. It has flow structures concentrated in its frontal area as well as pronounced escarpments. When they degrade, they can have depressions due to thermokarst.	(Ferrando et al., 2015; García et al., 2017; Gutiérrez Elorza, 2008; Serrano et al., 2011)
Valley rock glacier	Lobated or tongue-shaped debris body with interstitial ice that develop parallel to the axis of valleys. It has flow structures and scarps in frontal and lateral areas, caused by its viscous flow. In the study area, valley rock glaciers may have been derived from moraine deposits. They could persist in a fossil state without ice content.	(García et al., 2017; Gutiérrez Elorza, 2008; Janke et al., 2015; Ferrando et al., 2015)
Gelifluction lobes	Lobes, usually tongue-shaped, formed by downslope displacement of soils due to freeze–thaw action. They are common in periglacial environments. These landforms have occasionally been defined as solifluction lobes, although solifluction does not necessarily imply ice. García et al. (2017) defined gelifluction taluses as detrital slopes affected by transversal lobes caused by the freezing-thawing cycles generating the creeping of seasonally frozen ground.	(García et al., 2017; Huggett, 2007; Matsuoka, 2001)
Protalus lobe	Lobes that originate at the foot of a slope by the stacking of gelifluction deposits. In the Andes, they are associated to permafrost conditions. They have flow structures characterized by ridges and furrows transversal to the flow direction. These landforms have also been referred to as protalus ramparts. Their origin could also be related to debris slides over snowbanks.	(Ballantyne & Benn, 1994; García et al., 2017; Haeberli, 1985; Harrison et al., 2008; Whalley & Azizi, 2003)
Debris cone	Accumulation of reworked debris that falls from the slope. They are structured as cones or coalescences of debris cones (talus slope) that cover the bedrock or the till at the base of the valleys.	(Ballantyne, 2002)

4.1.1.2. Cirques. In the headwaters of all the valleys studied, groups of multiple cirques occur. Their diameters extend for 1–2 km. Cirques grade down-valley towards the glacial U-shaped valleys. Abrupt cirque walls can be up to 900 m in relief in the Río Hurtado sub-basin and up to 300 m in the Río Combarbalá sub-basin. Cirques are made up of rocky outcrops in the upper parts and colluvial slopes in the lower parts. Cirques at Río Hurtado have predominantly a southeast aspect, while cirques at Río Combarbalá generally present a southwest aspect. Topographic divides between cirques expose well-developed aretes and horns.

4.1.1.3. Ice-scoured bedrock. Ice-scoured bedrock areas were identified in the highest parts of the El Viento valley, between 3860 and 4070 m a.s.l. Here, the valley bottom appears as a topographic surface punctuated by glacially molded knobs. A darker layer of bedrock polished by the glacier is observed on the ice-scoured bedrock surface. The darker bedrock contrasts with the surrounding terrain covered by a thick mantle of glacial or gravitationally derived debris.

4.1.2. Glacial deposition

Accumulation landforms such as moraines and ridges are prominent in all the valleys. The mapping distinguishes two moraine belts (I and II) in El Toro, Las Arenas, and El Viento valleys, and five moraine belts (I-V) in El Despoblado valley (Table 2). We differentiate between two types of glaciogenic deposits. On the one hand, there are moraines ridges occurring as arcuate-shaped massive and relatively confined (<1 km wide) till deposits with a well-defined crest or sequence of crests. However, the most notable landform in terms of its extent corresponds to massive morainic terrain with irregular topography observed for moraine belt II, covering the bottom of all the studied valleys, classified here as hummocky moraine.

4.1.2.1. Moraines ridges. Lateral moraines are found down-valley on both sides of the El Viento, El Toro, and Las Arenas valleys, corresponding to moraine belt I. This moraine is preserved also down-valley at El Despoblado valley, but not within the area covered by our maps. This is a massive linear to arcuate-shaped ridge almost 2 km long, standing over up to

Table 2. Moraine deposit characteristics. The table contains data on the length of the moraine deposits in all the valleys, as well as the distance from the cirques, and the lower most limits that moraine deposits reach.

Moraine	Sub-basin	Valley	Length (km)	Distance from cirque (km)	Lower limit (m a.s.l.)
Moraine I	Río Hurtado	El Viento	2.0	10.0	3350
	Río Combarbalá	El Toro	2.8	6.0	2710
		Las Arenas	3.3	5.4	2970
Moraine II	Río Hurtado	El Despoblado	3.0	4.5	3600
		El Viento	9.6	7.9	3470
	Río Combarbalá	El Toro	9.0	3.7	3270
		Las Arenas	4.1	2.8	3320
Moraine III	Río Hurtado	El Despoblado	1.0	1.0	4230
Moraine IV	Río Hurtado	El Despoblado	0.1	0.1	4320
Moraine V	Río Hurtado	El Despoblado	0.05	0.05	4390

hundred meters above the valley bottom, with gentle slopes (15–20°), in some cases grading smoothly to the valley floor (Figure 2). These are wide-top moraines with faceted and sometimes striated boulders that may have a centimeter-scale weathered layer, such as in El Viento. Boulders are embedded in a granular surface and are abundant on the crest surface. In the Río Hurtado sub-basin, moraine I reaches the lower limit at ~3350 m a.s.l. and it is 10 km away from the cirques. In the Río Combarbalá sub-basin, moraine I reaches 2710 m a.s.l., ~6 km away from the cirques.

Lateral moraines also occur higher in El Viento, El Despoblado, and El Toro valleys, associated with moraine belt II. Lateral moraines II are 2–4 km long linear deposits on the margins of the valleys with faceted and sometimes striated boulders organized in a well-preserved crest on the top. In their proximal side, lateral moraines are made up by multiple arcuate-shaped ridges arranged parallel to each other (Figure 3).

Prominent 50 m high lateral moraines, which extend for as long as 1 km, are most likely preserved only in El Despoblado valley and represent the next drift generation, the moraine belt III. These moraine

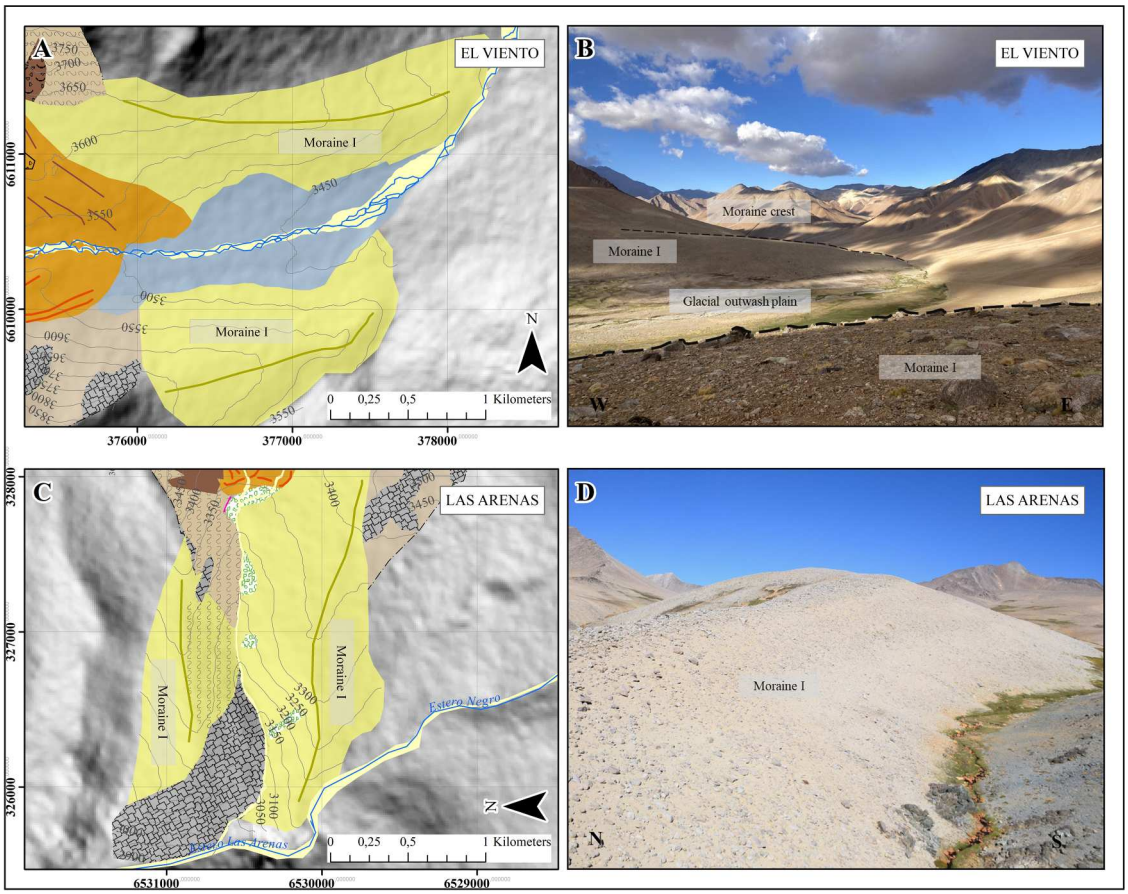

Figure 2. Map-photo pairs (A–B) and (C–D) of moraine I. (A) Detail of El Viento valley map to show moraine I at both sides of the valley separated by an outwash plain grading to moraine II (brown colored). For detailed legend refer to the main map in Supplementary Material. (B) Moraine I in El Viento. The image is taken from the top of the right lateral moraine I, looking down-valley. Moraine I in the background of the picture is an extensive deposit over hundred meters tall, as its counterpart at the other side of the valley (foreground). (C) Detail of Las Arenas valley map to show both lateral moraines I. (D) The southernmost moraine I in Las Arenas. The image is taken from the lower part of moraine I, looking up-valley. Maps scale is 1:20,000.

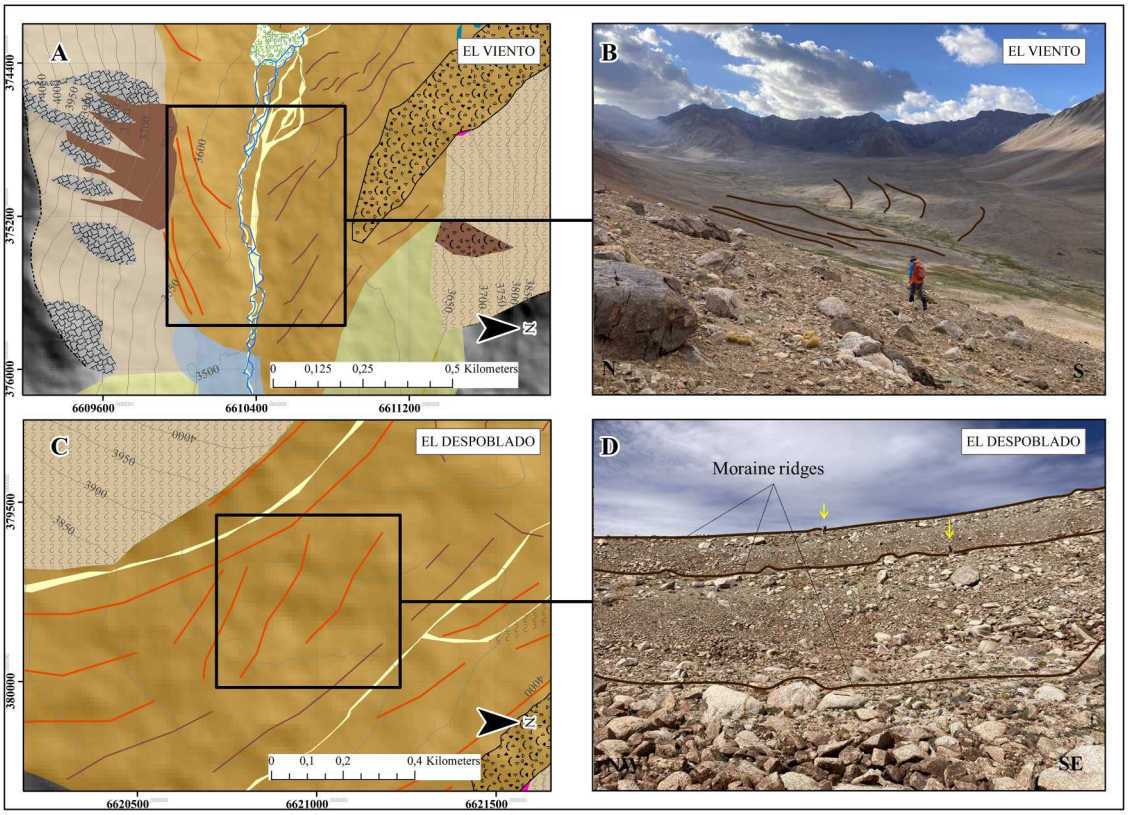

Figure 3. Map-photo pairs (A–B) and (C–D) of Moraine II. (A) Detail of El Viento valley map to show moraine II in its down-valley portion. For symbology refer to the main map in Supplementary Material. Black square is showing the area in the corresponding photo (B). (B) Image taken up-valley from the proximal slope of moraine I, showing successive moraine ridges (brown lines) superimposed to moraine II in El Viento valley. Cirques up-valley are shown in the background. (C) Detail of El Despoblado valley to show an up-valley portion of moraine II, close to one of the valley sides (right side). Black square is showing the area in the corresponding photo (D). (D) Stepped lateral moraine ridges in the eastern side of El Despoblado valley. The image is taken from the center of the valley and looking towards the right side of the valley. Moraine ridges are arranged in parallel and are decreasing in altitude towards the bottom of the image, indicating ice-thinning. Yellow arrows denote the positions of individuals on moraine ridges. Maps scale is 1:20,000.

ridges, found above 4230 m a.s.l., were built by former glacial lobes flowing simultaneously from different cirques, leaving behind arcuate-shaped lateral and medial moraines after retreat. Inboard of moraine III, small moraine arcs IV and V are at the foot of steep cirques walls in El Despoblado valley. Whereas the moraine arc IV is ~100 m from the cirques, reaching 4320 m a.s.l, the innermost moraine arc V is 50 m, reaching 4390 m a.s.l.

4.1.2.2. Hummocky moraine. A massive hummocky terrain composed of glaciogenic sediments was found in all studied valleys associated with moraine II. It appears as an irregular deposit that covers the valley bottom extensively, in some cases flanked by lateral moraine ridges and frontal smooth ramps (Figure 4(A)). This deposit is superimposed by arcuate ridges, sinkholes or thermokarst depressions, and debris-filled fractures. In addition, zone of debris accumulations more or less aligned with the top edge of topographic steps (escarpments) occur at the bottom of the valleys. These discrete boulderly zones may indicate positions where the ice stabilized due to a topographic control.

Arcuate ridges superimposed to the hummocky moraine are ~3–10 m high and ~100–200 m long (Figure 4(D)). These ridges are arranged successively in a stepped fashion and longitudinal regarding the main valley axis, although with slight curvatures towards the central area. Sinkholes of ~1–5 m diameter were mapped at moraine II in El Toro, El Viento, and specially in El Despoblado valleys. These features have been produced when the melting of buried ice triggers a supraglacial collapse preserved in the geomorphic record as fossil thermokarst (Figure 4(B)) (Fernández et al., 2022; Kjær & Krüger, 2001; Krüger et al., 2010; Miesen et al., 2021). Debris-filled fractures are also widespread on the hummocky moraines, such as in El Toro and El Despoblado valleys. These could be evidence of the accumulation of debris in tension cracks (Eyles, 1979; Fernández et al., 2022; Kjær & Krüger, 2001). Nonetheless, the debris-filled fractures may expose a patterned ground type of structure, which better resemble a cryoturbation effect (Figure 4(C)) (Matthews et al., 1998).

Sinkholes and, in some cases, debris-filled fractures are evidence for ice stagnation and *in situ* deglaciation,

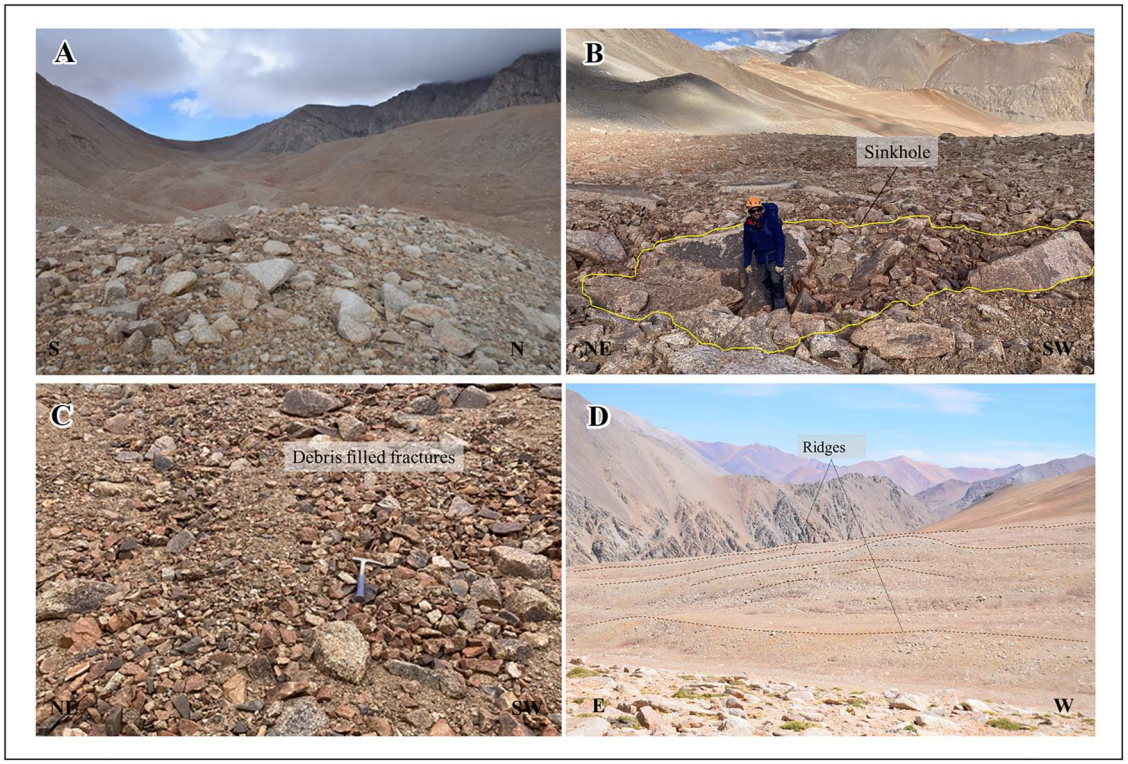

Figure 4. Hummocky moraine features. (A) General view of hummocky moraine II in El Despoblado. (B) Fossil thermokarst (sinkhole) overprinting hummocky moraine II at El Despoblado. (C) Debris-filled fractures in moraine II, El Despoblado valley. Geologic hammer for scale and located within the debris-filled fracture. (D) Ridges overprinting hummocky moraine II at El Despoblado valley. They are arranged successively and parallel to the direction of ice flow although with slight curvatures towards the internal area of the valley.

known as down-wasting (Kjær & Krüger, 2001). Periods of negative mass balance produce debris-covered glacier snouts, frontal stagnation, and down-wasting (Fernández et al., 2022; García et al., 2014; Krüger et al., 2010). The inactive debris-covered snout is then detached from the active glacier, giving place to ice-cored moraines, which evolve into dead-ice deposits when these ice bodies have melted completely (Fernández et al., 2022; Moore, 2021). Thus, the hummocky moraine is the final stage of a de-icing progression after the *in situ* collapse of debris-covered ice in response to a warming/drying climate period (Bartlett et al., 2021; Fernández et al., 2022). On the other hand, successive arcuate stepped ridges punctuating the hummocky moraine resemble former active ice margins capable of building lateral and latero-frontal moraine ridges during overall glacier demise. Therefore, the hummocky moraine is a mosaic of glacial and deglacial features, with glacier re-advances reworking till previously deposited into ridges that separate active versus inactive ice. Hummocky moraines have also been interpreted as a consequence of thrusting, nonetheless we do not observe any of the features expected for this mechanism in our study area (Hambrey et al., 1997; Lukas, 2005). We acknowledge that the lack of sediment stratigraphic sections in the studied valleys does not help to better study this alternative interpretation.

4.2. Periglacial geomorphology

Periglacial landforms such as rock glaciers, and gelifluction and protalus lobes overprinting valley slopes and moraines were identified in the study area. These landforms are more abundant above 3700 m a.s.l. and in association with south-facing slopes in the case of rock glaciers and south to southwestern facing slopes in the cases of gelifluction and protalus lobes. There is a greater dominance of periglacial landforms in the valleys of Río Hurtado sub-basin, where altitudes are higher. Some of these landforms can be seen as clear indicators for the current or former presence of permafrost.

4.2.1. Gelifluction lobes

Gelifluction lobes were identified on detrital slopes of 20–30° between 3320 and 4500 m a.s.l. They are elongated lobes oriented transversal to the direction of the slope on *in situ* detrital slopes with a southwest aspect (Figure 5(A,B)). Gelifluction lobes were also observed on moraine deposits, mainly in unit II in the El Despoblado valley (Figure 5(A)). These features appear commonly on the proximal sides of lateral moraines with slopes of ~20°. The gelifluction lobes on moraine deposits increase in frequency toward the cirques.

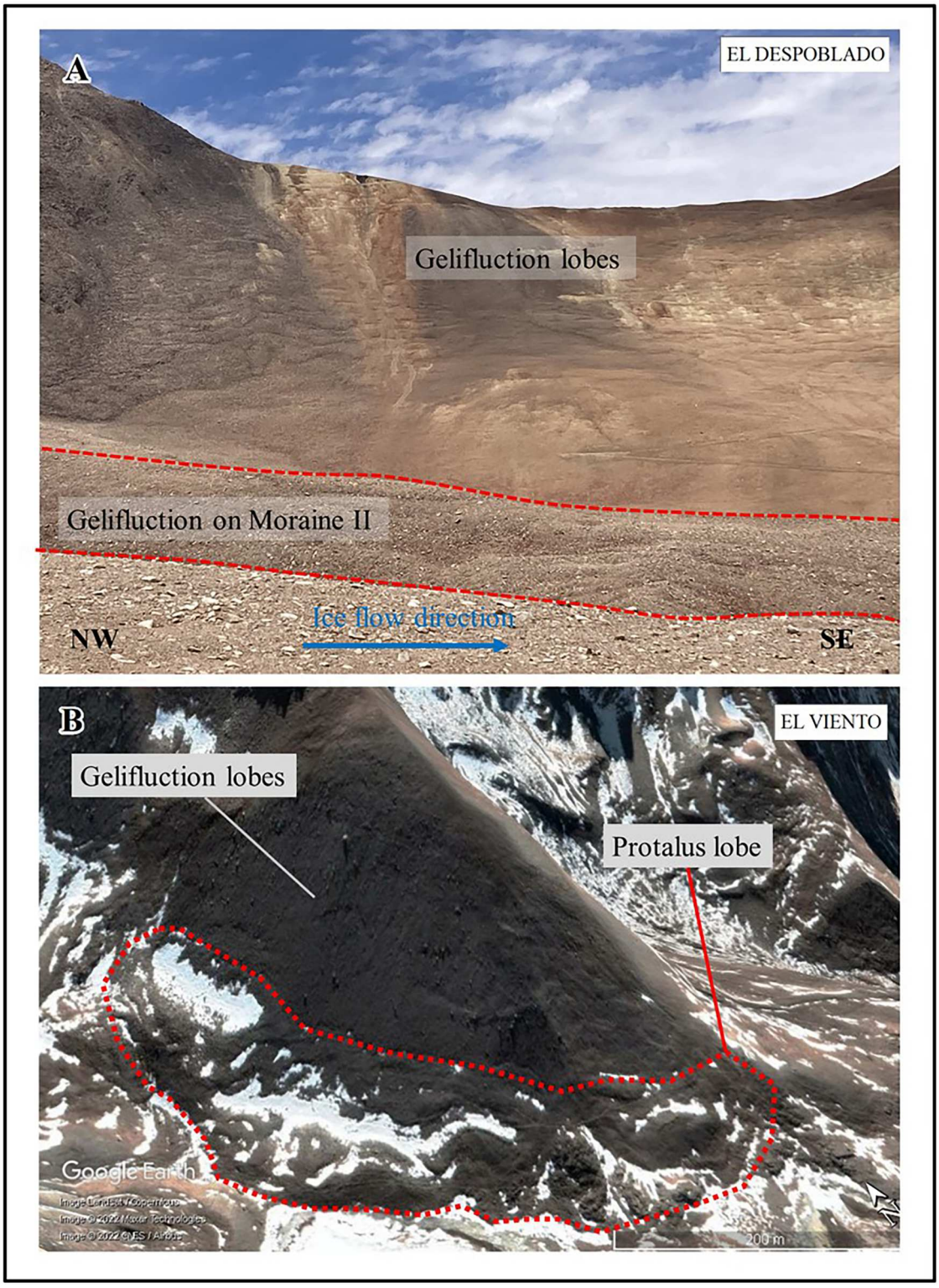

Figure 5. Gelifluction and protalus lobes. (A) Gelifluction lobes occur on the left slope of El Despoblado valley (background). Gelifluction lobes are also affecting moraine II deposits (foreground) (B) Google Earth's satellite image showing protalus lobes at the foot of a slope overprinted by gelifluction lobes in El Viento valley. The slope varies from 25° in its upper part, to 15° where the protalus lobes are being formed.

4.2.2. Protalus lobes

Protalus lobes were identified at the foot of talus or detrital slopes in the area where the slope decreases from 25°–30° to around 15°. The effect of the change in slope causes the stacking of the lobes and, consequently, the formation of the protalus lobe (García et al., 2017; Haeberli, 1985), which are larger lobes compared to gelifluction lobes and have steep fronts. They are typically formed at short distances from the headwall (Figure 5(B)). Protalus lobes are found between 3300 and 4050 m a.s.l in both valleys of the Río Hurtado subbasin and in the Las Arenas valley.

4.2.3. Rock glaciers

Rock glaciers are a major geomorphic indicator for the occurrence of permafrost conditions, as they are a visible expression of the creeping of mountain permafrost (Barsch, 1992; Buckel et al., 2021). Most of them are talus rock glaciers forming at the lower parts of debris cones in cirques. Rock glaciers are rarely found covering cirques in all their extent, which are known as cirque rock glaciers (García et al., 2017; Gutiérrez Elorza, 2008). In contrast, there are relatively few larger rock glaciers covering the valley bottoms.

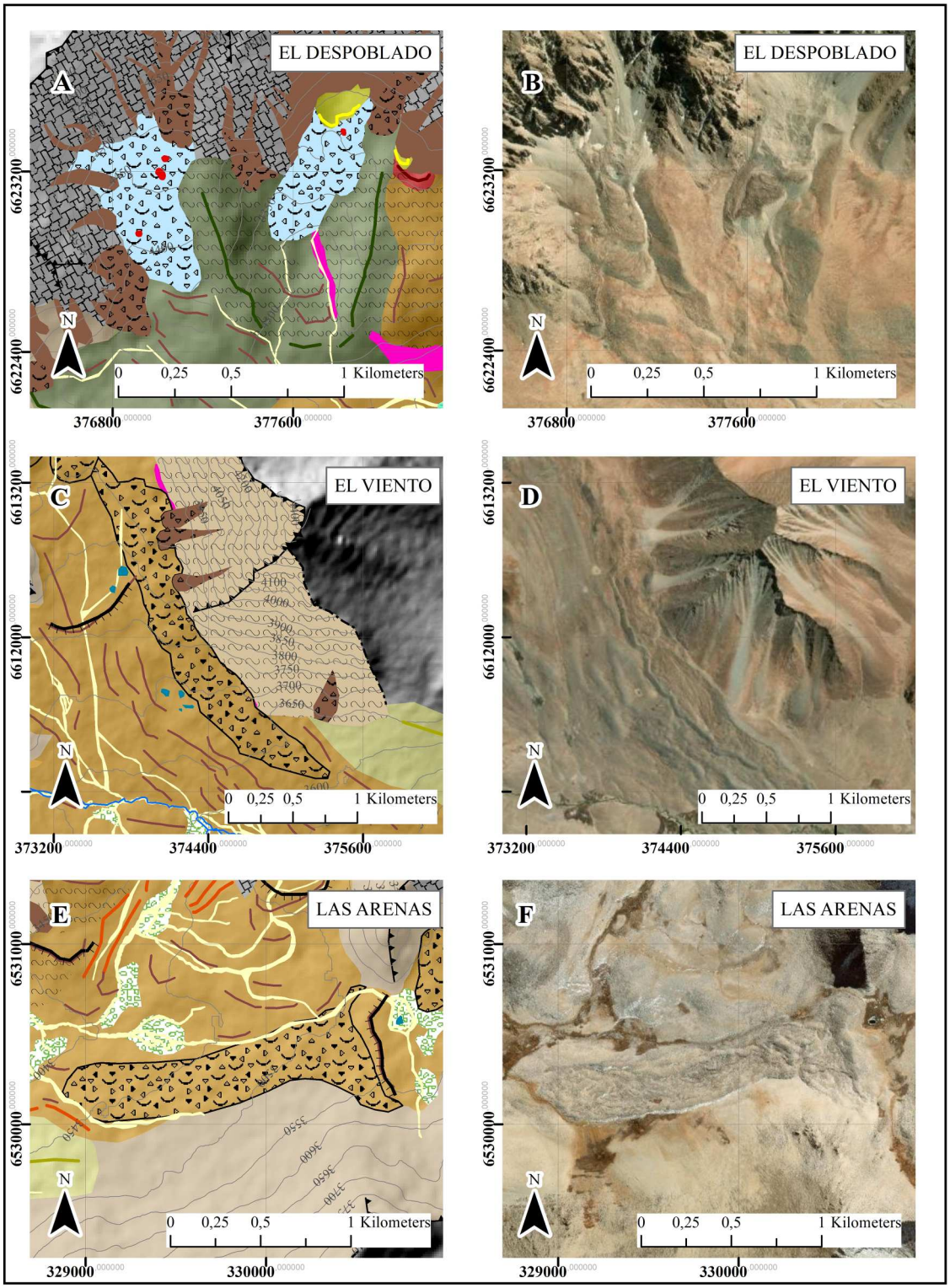

Figure 6. Rock glaciers. (A) Detail of El Despoblado valley map showing cirque rock glaciers. Note the presence of a small thermokarst depression on the rock glacier surface. ESRI Base Map image at the right (B) covers the same area as (A) and allows describing the flow structures of rock glaciers. (C) Detail of valley rock glacier at El Viento valley. ESRI Base Map at the right (D) comprises the same area. (E) Detail of Las Arenas valley showing valley rock glacier. To the right, ESRI Base Map image (F) covers the same area. Maps scale is 1:20,000.

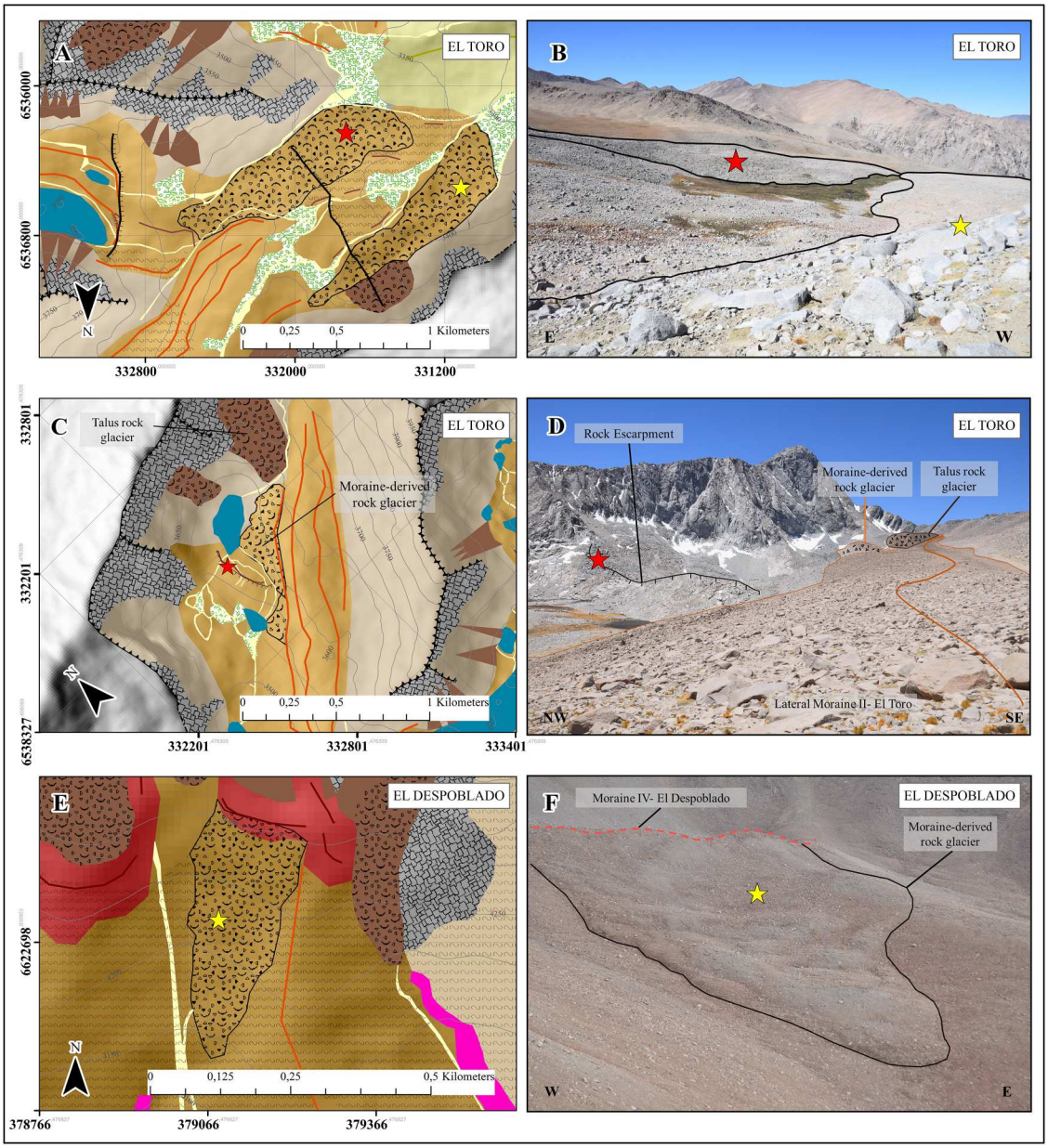

Figure 7. Map-photo pairs of moraine-derived rock glaciers (A–B; C–D: E–F). (A) Detail of El Toro valley map showing moraine-derived rock glaciers. Map scale is 1:15,000. (B) Photo of the moraine-derived rock glaciers of El Toro valley shown in (A), view is down-valley. (C) Detail of El Toro valley map showing moraine-derived rock glacier formed from the sediments of lateral moraine II. Red star is showing an escarpment in the valley. Map scale is 1:15,000. (D) Photo taken up-valley from lateral moraine II in El Toro valley to show the area comprised in the map in (C). Brown line represents the moraine II crest. (E) Detail of El Despoblado valley map to show a moraine-derived rock glacier. Map scale is 1:4500. (F) Photo taken up-valley to show moraine-derived rock shown in (E).

In our study area, talus rock glaciers have steep fronts that exceed 10 meters in height. These are wider features characterized by a relatively small longitudinal extent (70–100 m) compared with their transversal size (100–170 m). When the longitudinal development is greater, surpassing the slopes and superimposing on the bottom of the valley, the landforms typically present some flow structures, such as ridges and transversal furrows, which are formed when the flow is disturbed by a decrease in slope (Loewenherz et al., 1989). On occasions, coalescences between talus rock glaciers at the base of contiguous talus accumulations can occur, extending transversally for a kilometer, such as in El Viento valley.

Two cirque rock glaciers were identified in El Despoblado valley where altitudes exceed 4200 m a.s.l. (Figure 6(A)). Both rock glaciers seem to arise from the walls of the cirques, although the one to the west could be emanating from the distal slope of moraine V and therefore be described as a 'debris rock glacier' (Barsch, 1988; Hughes et al., 2003). Our current observations prevent definitive conclusions at present. Cirque rock glaciers are tongue-shaped with lengths reaching 800 m, while their widths reach 400 m.

Figure 8. Debris cones. (A) Debris cones in El Ternero valley as viewed from where moraine II at El Despoblado merges with the one in El Ternero valley. The debris cones are arranged at the left slope of El Ternero valley. The dotted red line helps to visualize that these cones have similar heights as the lateral moraine II. El Ternero valley includes conspicuous lateral moraine, indicating that the valley was formerly glaciated. Once deglaciated debris cones formed linked to paraglacial adjustment. (B) Talus rock glacier formed at the toe of debris cones in the El Ternero valley.

These landforms present steep (25°) and high (50 m) fronts. Their surface presents obvious flow structures with notorious ridges as well as transverse and longitudinal furrows. They can present depressions on their surfaces suggesting buried ice (Figure 6(A)).

A valley-type rock glacier occurs in El Viento valley (Figure 6(B)). This tongue-shaped feature develops for 3 km to the south of the valley until 3500 m a.s.l, today disconnected to any source of debris (e.g. cirques, slopes, or glaciers). Its width reaches 400 m. The landform presents steep sides with greater relief on its eastern walls (~50 m), adjacent to the valley slopes, compared to its western walls (~25 m), where the landform adjoins the hummocky moraine II

topography. Throughout its length, degraded flow structures marked by ridges and furrows are present, different from those well-pronounced of cirque rock glaciers. A valley-type rock glacier morphology is also observed in Las Arenas valley (Figure 6(C)). This tongue-shaped, rocky-surface landform extends for 1.7 km down to 3400 m a.s.l. and has a width of 350 m. Its right slope, which has a height of around 10 m and a slope of 15°, converges with the hummocky moraine II topography in this valley. This valley rock glacier also shows subdued flow structures suggesting that it is currently not flowing and, thus, it seems to be inactive (Janke et al., 2015) possibly indicating formation when climatic conditions allowed permafrost to occur at lower elevations than today.

4.2.4. Moraine-derived rock glaciers

Rock glaciers originating from glacial deposits were mapped in El Despoblado and El Toro valleys (Figure 7). These rock glaciers occur where the slope is steep enough to have allowed viscous flow of ice within a moraine matrix and thus the development of a type of 'debris rock glacier' (e.g. Barsch, 1996) or moraine-derived rock glacier (Lilleøren & Etzelmüller, 2011). A good example is the hummocky moraine II in El Toro valley. Here, two of these moraine-derived rock glaciers occur. These tongue-shaped features have a length of approximately 900 m and a width of ~300 m and develop until 3300 m a.s.l. They develop in an area where the topography of the valley presents an escarpment, which favored in the past the landform creeping. Sometimes, the stacking of gelifluction lobes at the base of moraine deposits can develop small rock glaciers.

4.3. Paraglacial geomorphology

Landforms which formation is influenced by paraglacial conditions, referring to the period immediately following a glacial retreat, were recognized. These are associated with non-glacial processes, but their formation is determined by glacial-deglacial sequences (Church & Ryder, 1972). The paraglacial period has an effect on the glaciated rock walls when the withdrawal of glaciers exposes these rock walls resulting in their 'debuttressing' (Ballantyne, 2002). Thus, processes associated with the stress-relief of rock walls, such as rockfalls, are exacerbated favoring talus slope accumulations, including debris cones (Ballantyne, 2002; Wyrwoll, 1977).

4.3.1. Debris cones

Debris cones were observed on the valley slopes. These conical features are typically formed at south-facing slopes, above ~3800 m a.s.l. They are conformed of well-organized debris, with the largest boulders being found at the toe of the cones. Their height is around 180 m and their width at the base around 60 m. They are organized as a succession of cones with similar apex heights forming talus slopes. The set of cones can extend uninterruptedly for almost 2 km. The height of the apex of the landforms may coincide with the estimated height of lateral moraines II. This is notorious where moraine II of El Despoblado valley merges into the lateral side of the El Ternero main valley, where a sequence of talus cones is well developed (Figure 8(A)) until the end of the valley. There, a prominent lateral moraine rises. This indicates that the talus cones postdate ice retreat and can be linked to slope relaxation and associated gravitational processes (Ballantyne, 2002; Wyrwoll, 1977).

5. Conclusions

The geomorphic record of the Andean Río Limarí basin is composed by a mosaic of mountain landforms accounting for a long-term evolution of the cryosphere, including glacial, paraglacial, and periglacial processes. The presence of faceted and striated boulders, together with well-developed lateral moraine ridges, and in the light of the records in the region, demonstrate that the studied valleys were occupied by Late Pleistocene glaciers, which during deglaciation were highly covered by debris to then evolve into dead-ice moraines.

Up to five moraine belts (I–V) are mapped in the study area (e.g. El Despoblado valley). Their position nicely represents the main glacial advances for the region and their extents. The lateral moraines of unit I indicate the larger glacial advance preserved in the Limarí basin. The extent of moraine II indicates a prominent glacial advance followed by a deglaciation process marked mostly by *in situ* ice thinning but interrupted by ice re-advances. After this main advance and retreat phases, glaciers experimented several minor re-advances probably until as recent as the Late Holocene, as evidenced by fresh moraine deposits in El Despoblado valley (moraines III, IV, and V).

Periglacial landforms, such as rock glaciers, gelifluction lobes, and protalus lobes, are widespread in the study area, in particular in the Río Hurtado sub-basin. These landforms have affected the glacial deposits, leading to complex periglacial landforms such as 'debris rock glaciers' or moraine-derived rock glaciers.

More chronological and detailed morpho-stratigraphic research is needed to constrain the cryosphere evolution and associated climate changes linked to the geomorphic record we have presented in this paper.

Software

Geomorphological mapping was conducted using ArcGIS 10.8.1 software. With this software, image

processing and analysis were carried out using ESRI Base Map image as a reference for the digitization of point, polylines, and polygons shapefiles. Google Earth Pro was also used for the image analysis and shapefile creation.

Geolocation information

The study area presented within these maps is located between the following coordinates:

70°10′0″ W – 70°52′0″ W; 30°29′0″ S – 31°22′0″ S.

Acknowledgements

Javiera Carraha acknowledges the Instituto de Geografía, Pontificia Universidad Católica de Chile since this research is developed for a thesis within the Doctorado en Geografía program, and for providing the license to ArcGIS 10.8.1 software. We acknowledge Wilfried Haeberli for discussion on this geomorphological record. We also thank Diego Romero and Roberto Merino for their assistance during fieldwork, as well as Hacienda El Bosque for facilitating access to the study area. This work was supported by the Fondo Nacional de Desarrollo Científico y Tecnológico [FONDECYT] under Grant [#1200935] awarded to Juan-Luis García. Samuel U. Nussbaumer and Juan-Luis García acknowledge support from the Swiss National Science Foundation (project IZSEZ0_215412). We sincerely thank the three reviewers, María-Victoria Soto, Philip Hughes, and Jessica Baker, as well as the scientific editor for their valuable feedback that greatly improved the paper.

Disclosure statement

No potential conflict of interest was reported by the author(s).

Funding

This work was supported by Fondo Nacional de Desarrollo Científico y Tecnológico (FONDECYT) [grant number #1200935]; Swiss National Science Foundation [IZSEZ0_215412].

Data availability statement

The data that support the findings of this study are available from the corresponding author, Javiera Carraha, upon reasonable request.

References

Aguilar, G., Riquelme, R., Lohse, P., Cabré, A., García, J.-L., Aguilar, G., Riquelme, R., Lohse, P., Cabré, A., & García, J.-L. (2022). Chronology of glacial advances and deglaciation in the Encierro River Valley (29° Lat. S), Southern Atacama Desert, based on geomorphological mapping and cosmogenic 10Be exposure ages. *Frontiers in Earth Science*, *10*(878318). https://doi.org/10.3389/FEART.2022.878318

Anderson, L. S., Roe, G. H., & Anderson, R. S. (2014). The effects of interannual climate variability on the moraine record. *Geology*, *42*(1), 55–58. https://doi.org/10.1130/G34791.1

Anderson, R. S., Anderson, L. S., Armstrong, W. H., Rossi, M. W., & Crump, S. E. (2018). Glaciation of alpine valleys: The glacier – debris-covered glacier – rock glacier continuum. *Geomorphology*, *311*, 127–142. https://doi.org/10.1016/j.geomorph.2018.03.015

Anderson, R. S., & Anderson, S. P. (2010). *Geomorphology: The mechanics and chemistry of landscapes*. Cambridge University Press.

Azócar, G. F., & Brenning, A. (2010). Hydrological and geomorphological significance of rock glaciers in the dry Andes, Chile (27°-33°S). *Permafrost and Periglacial Processes*, *21*(1), 42–53. https://doi.org/10.1002/ppp.669

Ballantyne, C. K. (2002). Paraglacial geomorphology. *Quaternary Science Reviews*, *21*(18–19), 1935–2017. https://doi.org/10.1016/S0277-3791(02)00005-7

Ballantyne, C. K., & Benn, D. I. (1994). Glaciological constraints on protalus rampart development. *Permafrost and Periglacial Processes*, *5*(3), 145–153. https://doi.org/10.1002/ppp.3430050304

Barsch, D. (1988). Rock glaciers. In M. Clark (Ed.), *Advances in periglacial geomorphology* (pp. 69–90). Wiley.

Barsch, D. (1992). Permafrost creep and rockglaciers. *Permafrost and Periglacial Processes*, *3*(3), 175–188. https://doi.org/10.1002/ppp.3430030303

Barsch, D. (1996). *Rockglaciers: Indicators for the present and former geoecology in high mountain environments* (Vol. 16, pp. XIV–331). Springer.

Bartlett, O. T., Ng, F. S. L., & Rowan, A. V. (2021). Morphology and evolution of supraglacial hummocks on debris-covered Himalayan glaciers. *Earth Surface Processes and Landforms*, *46*(3), 525–539. https://doi.org/10.1002/esp.5043

Bendle, J. M., Palmer, A. P., Thorndycraft, V. R., & Matthews, I. P. (2017). High-resolution chronology for deglaciation of the Patagonian Ice Sheet at Lago Buenos Aires (46.5°S) revealed through varve chronology and Bayesian age modelling. *Quaternary Science Reviews*, *177*, 314–339. https://doi.org/10.1016/j.quascirev.2017.10.013

Benn, D. I., & Evans, D. J. A. (2010). *Glaciers and glaciation* (2nd ed.). Hodder Education.

Benn, D. I., & Owen, L. A. (2002). Himalayan glacial sedimentary environments: A framework for reconstructing and dating former glacial extents in high mountain regions. *Quaternary International*, *97/98*, 3–25. https://doi.org/10.1016/S1040-6182(02)00048-4

Brenning, A. (2005). Geomorphological, hydrological and climatic significance of rock glaciers in the Andes of central Chile (33-35 S). *Permafrost and Periglacial Processes*, *16*, 231–240. https://doi.org/10.1002/ppp.528

Brenning, A., & Trombotto, D. (2006). Logistic regression modeling of rock glacier and glacier distribution: Topographic and climatic controls in the semi-arid Andes. *Geomorphology*, *81*(1-2), 141–154. https://doi.org/10.1016/j.geomorph.2006.04.003

Buckel, J., Reinosch, E., Voigtländer, A., Dietze, M., Bücker, M., Krebs, N., Schroeckh, R., Mäusbacher, R., & Hördt, A. (2022). Rock glacier characteristics under semiarid climate conditions in the western Nyainqêntanglha range, Tibetan Plateau. *Journal of Geophysical Research: Earth Surface*, *127*(1), e2021JF006256. https://doi.org/10.1029/2021JF006256

Capps, S. (1910). Rock glaciers in Alaska. *The Journal of Geology*, *18*(4), 359–375. https://doi.org/10.1086/621746

Carrasco, J. F., Casassa, G., & Quintana, J. (2005). Changes of the 0°C isotherm and the equilibrium line altitude in central Chile during the last quarter of the 20th century. *Hydrological Sciences Journal*, *50*(6), 933–948. https://doi.org/10.1623/hysj.2005.50.6.933

Caviedes, C., & Paskoff, R. (1975). Quaternary glaciations in the Andes of north-central Chile. *Journal of Glaciology*, *14* (70), 155–170. https://doi.org/10.3189/S0022143000013472

Charrier, R., Iturrizaga, L., Carretier, S., & Regard, V. (2019). Geomorphologic and glacial evolution of the Cachapoal and southern Maipo catchments in the Andean Principal Cordillera, central Chile (34 ° -35° S). *Andean Geology*, *46*(2), 240–278. https://doi.org/10.5027/andgeoV46n2-3108

Church, M., & Ryder, J. M. (1972). Paraglacial sedimentation: A consideration of fluvial processes conditioned by Glaciation. *GSA Bulletin*, *83*(10), 3059–3072. https://doi.org/10.1130/0016-7606(1972)83[3059:PSACOF]2.0.CO;2

Clark, D. H., Steig, E. J., Potter, N., & Gillespie, A. R. (1998). Genetic variability of rock glaciers. *Geografiska Annaler: Series A, Physical Geography*, *80*(3–4), 175–182. https://doi.org/10.1111/j.0435-3676.1998.00035.x

DGA-Dirección General de Aguas. (2022). *Inventario Público de Glaciares*. Unidad de Glaciología y Nieves, Dirección General de Aguas. Ministerio de Obras Públicas.

Evans, I. S., & Cox, N. J. (1974). Geomorphometry and the operational definition of cirques. *Area*, *6*, 150–153.

Eyles, N. (1979). Facies of supraglacial sedimentation on Icelandic and Alpine temperate glaciers. *Canadian Journal of Earth Sciences*, *16*(7), 1341–1361. https://doi.org/10.1139/E79-121

Fernández, H., García, J.-L., Nussbaumer, S. U., Geiger, J., Gärtner-Roer, I., Pérez, F., Tikhomirov, D., Christl, M., & Egli, M. (2022). De-icing landsystem model for the Universidad Glacier (34° S) in the Central Andes of Chile during the past ~660 years. *Geomorphology*, *400*, 108096. https://doi.org/10.1016/j.geomorph.2021.108096

Fernández-Navarro, H., García, J. L., Nussbaumer, S. U., Tikhomirov, D., Pérez, F., Gärtner-Roer, I., Christl, M., & Egli, M. (2023). Fluctuations of the Universidad Glacier in the Andes of central Chile (34° S) during the latest Holocene derived from a 10Be moraine chronology. *Quaternary Science Reviews*, *300*, 107884. https://doi.org/10.1016/j.quascirev.2022.107884

Ferrando, F. A., & Sarricolea, P. (2020). *Permafrost has support of run-off in a semiarid region, Chile:* "*cochiguaz*". River Sub-Basin Rock Glaciers, Warming & Mining Impact. First Southern Hemisphere Conference on Permafrost, Queenstown, New Zealand, 4–14 December, 2019.

Ferrando, F. J., Janke, J. R., & Bellisario, A. C. (2015). Clasificación de glaciares rocosos de origen glacial. *Anales de La Sociedad Chilena de Ciencias Geográficas*, 33–41.

García, A., Ulloa, C., Amigo, G., Milana, J. P., & Medina, C. (2017). An inventory of cryospheric landforms in the arid diagonal of South America (high Central Andes, Atacama region, Chile). *Quaternary International*, *438*, 4–19. https://doi.org/10.1016/j.quaint.2017.04.033

García B., J.-L., Pizarro M., F. I., & Calcagni R., V. (2014). Fluctuaciones glaciales holocénicas en el Cajón del Maipo, Andes centrales de Chile: observaciones morfoestratigráficas de los glaciares Loma Larga y Nieves Negras. In A. Borsdorf, R. Sánchez, R. Hidalgo, & H. M. Zunino (Eds.), *Los riesgos traen oportunidades: Transformaciones globales en Los Andes sudamericanos* (pp. 35–52). Serie GEOlibros. https://www.researchgate.net/publication/267268320.

Garreaud, R. D. (2009). The Andes climate and weather. *Advances in Geosciences*, *22*, 3–11. https://doi.org/10.5194/adgeo-22-3-2009

Garreaud, R. D., Boisier, J. P., Rondanelli, R., Montecinos, A., Sepúlveda, H. H., & Veloso-Aguila, D. (2020). The central Chile Mega Drought (2010–2018): A climate dynamics perspective. *International Journal of Climatology*, *40*(1), 421–439. https://doi.org/10.1002/joc.6219

Giardino, J. R., & Vitek, J. D. (1988). The significance of rock glaciers in the glacial periglacial landscape continuum. *Journal of Quaternary Science*, *3*(1), 97–103. https://doi.org/10.1002/jqs.3390030111

Gordon, J. E. (1981). Ice-scoured topography and Its relationships to bedrock structure and ice movement in parts of northern Scotland and west Greenland. *Geografiska Annaler. Series A, Physical Geography*, *63*(1/2), 55–65. https://doi.org/10.2307/520564

Gutiérrez Elorza, M. (2008). *Geomorfología*. Pearson Prentice Hall.

Haeberli, W. (1985). Creep of mountain permafrost: Internal structure and flow of Alpine rock glaciers. In Daniel Vischer (Ed.), *Mitteilungen der Versuchsanstalt für Wasserbau, Hydrologie und Glazialogie* (Vol. 77, pp. 1–142). Eidgenössische Technische Hochschule Zürich.

Haeberli, W., & Beniston, M. (1998). Climate change and its impacts on glaciers and permafrost in the Alps. *Ambio*, *27*(4), 258–265.

Hambrey, M. J., Huddart, D., Bennett, M. R., & Glasser, N. F. (1997). Genesis of hummocky moraines" by thrusting in glacier ice: Evidence from Svalbard and Britain. *Journal of the Geological Society*, *154*(4), 623–632. https://doi.org/10.1144/gsjgs.154.4.0623

Harrison, S., Whalley, B., & Anderson, E. (2008). Relict rock glaciers and protalus lobes in the British Isles: Implications for Late Pleistocene Mountain geomorphology and palaeoclimate. *Journal of Quaternary Science*, *23* (3), 287–304. https://doi.org/10.1002/jqs.1148

Huggett, R. J. (2007). *Fundamentals of geomorphology* (2nd ed., pp. 1–488). Routledge Fundamentals of Physical Geography. https://doi.org/10.4324/9780203947111.

Hughes, P. D. (2010). Geomorphology and quaternary stratigraphy: The roles of morpho-, litho-, and allostratigraphy. *Geomorphology*, *123*(3–4), 189–199. https://doi.org/10.1016/j.geomorph.2010.07.025

Hughes, P. D., Gibbard, P. L., & Woodward, J. C. (2003). Relict rock glaciers as indicators of Mediterranean palaeoclimate during the Last Glacial Maximum (Late Würmian) in northwest Greece. *Journal of Quaternary Science*, *18*(5), 431–440. https://doi.org/10.1002/jqs.764

Hughes, P. D., Gibbard, P. L., & Woodward, J. C. (2005). Quaternary glacial records in mountain regions: A formal stratigraphical approach. *Episodes*, *28*(2), 85–92. https://doi.org/10.18814/EPIIUGS/2005/V28I2/002

Janke, J. R., Bellisario, A. C., & Ferrando, F. A. (2015). Classification of debris-covered glaciers and rock glaciers in the Andes of central Chile. *Geomorphology*, *241*, 98–121. https://doi.org/10.1016/j.geomorph.2015.03.034

Kjær, K. H., & Krüger, J. (2001). The final phase of dead-ice moraine development: Processes and sediment architecture, Kötlujökull, Iceland. *Sedimentology*, *48*(5), 935–952. https://doi.org/10.1046/j.1365-3091.2001.00402.x

Knight, J. (2019). A new model of rock glacier dynamics. *Geomorphology*, *340*, 153–159. https://doi.org/10.1016/j.geomorph.2019.05.008

Knight, J., & Harrison, S. (2014). Mountain glacial and paraglacial environments under global climate change: Lessons from the past, future directions and policy implications. *Geografiska Annaler: Series A, Physical Geography*, *96*(3), 245–264. https://doi.org/10.1111/geoa.12051

Knight, J., Harrison, S., & Jones, D. B. (2019). Rock glaciers and the geomorphological evolution of deglacierizing mountains. *Geomorphology*, *324*, 14–24. https://doi.org/10.1016/j.geomorph.2018.09.020

Krüger, J., Kjær, K. H., & Schomacker, A. (2010). Dead-ice environments: A landsystems model for a debris-charged, stagnant lowland glacier margin, Kötlujökull. *Developments in Quaternary Science*, *13*, 105–126. https://doi.org/10.1016/S1571-0866(09)01307-4

Lilleøren, K. S., & Etzelmüller, B. (2011). A regional inventory of rock glaciers and ice-cored moraines in Norway. *Geografiska Annaler: Series A, Physical Geography*, *93*(3), 175–191. https://doi.org/10.1111/J.1468-0459.2011.00430.X

Lira, M. P., García, J. L., Bentley, M. J., Jamieson, S. S. R., Darvill, C. M., Hein, A. S., Fernández, H., Rodés, Á, Fabel, D., Smedley, R. K., & Binnie, S. A. (2022). The last glacial maximum and deglacial history of the Seno Skyring Ice Lobe (52°S), Southern Patagonia. *Frontiers in Earth Science*, *10*, 892316. https://doi.org/10.3389/feart.2022.892316

Loewenherz, D., Lawrence, C., & Weaver, R. (1989). On the development of transverse ridges on rock glaciers. *Journal of Glaciology*, *35*(121), 383–391. https://doi.org/10.3189/S002214300000931X

Lukas, S. (2005). A test of the englacial thrusting hypothesis of "hummocky" moraine formation: Case studies from the northwest Highlands, Scotland. *Boreas*, *34*(3), 287–307. https://doi.org/10.1111/J.1502-3885.2005.TB01102.X

Mackintosh, A. N., Anderson, B. M., & Pierrehumbert, R. T. (2017). Reconstructing climate from glaciers. *Annual Review of Earth and Planetary Sciences*, *45*(1), 649–680. https://doi.org/10.1146/annurev-earth-063016-020643

Matsuoka, N. (2001). Solifluction rates, processes and landforms: A global review. *Earth-Science Reviews*, *55*(1-2), 107–134. https://doi.org/10.1016/S0012-8252(01)00057-5

Matthews, J. A., Shakesby, R. A., Berrisford, M. S., & McEwen, L. J. (1998). Periglacial patterned ground on the Styggedalsbreen glacier foreland, Jotunheimen, southern Norway: Micro-topographic, paraglacial and geoecological controls. *Permafrost and Periglacial Processes*, *9*(*2*), 147–166. https://doi.org/10.1002/(SICI)1099-1530(199804/06)9:2<147::AID-PPP278>3.0.CO;2-9

May, J.-H., Zech, R., Schellenberger, A., Kull, C., & Veit, H. (2011). Quaternary environmental and climate changes in the Central Andes. *Cenozoic Geology of the Central Andes of Argentina, SCS Publications*, 247–263.

Miesen, F., Dahl, S. O., & Schrott, L. (2021). Evidence of glacier-permafrost interactions associated with hydro-geomorphological processes and landforms at Snøhetta, Dovrefjell, Norway. *Geografiska Annaler: Series A, Physical Geography*, *103*(3), 273–302. https://doi.org/10.1080/04353676.2021.1955539

Monnier, S., & Kinnard, C. (2012). From "true" glaciers to rock glaciers? The case of the Llanos la Liebre rock glacier, dry Andes of Chile. *Geophysical Research Abstracts*, *14*, 1–1.

Monnier, S., & Kinnard, C. (2015). Reconsidering the glacier to rock glacier transformation problem: New insights from the central Andes of Chile. *Geomorphology*, *238*, 47–55. https://doi.org/10.1016/j.geomorph.2015.02.025

Monnier, S., & Kinnard, C. (2017). Pluri-decadal (1955–2014) evolution of glacier-rock glacier transitional landforms in the central Andes of Chile (30–33° S). *Earth Surface Dynamics*, *5*(3), 493–509. https://doi.org/10.5194/esurf-5-493-2017

Monnier, S., Kinnard, C., Surazakov, A., & Bossy, W. (2014). Geomorphology, internal structure, and successive development of a glacier foreland in the semiarid Chilean Andes (Cerro Tapado, upper Elqui Valley, 30°08′ S., 69° 55′ W.). Geomorphology 207, 126–140. https://doi.org/10.1016/j.geomorph.2013.10.031

Moore, P. L. (2021). Numerical simulation of supraglacial debris mobility: Implications for ablation and landform genesis. *Frontiers in Earth Science*, *9*, 595. https://doi.org/10.3389/FEART.2021.710131/BIBTEX

Morén, B., Heyman, J., & Stroeven, A. P. (2011). Glacial geomorphology of the central Tibetan Plateau. *Journal of Maps*, *7*(1), 115–125. https://doi.org/10.4113/jom.2011.1161

Paskoff, R. (1977). Quaternary of Chile: The state of research. *Quaternary Research*, *8*(1), 2–31. https://doi.org/10.1016/0033-5894(77)90054-0

Quintana, J. M., & Aceituno, P. (2012). Changes in the rainfall regime along the extratropical west coast of South America (Chile): 30-43° S. *Atmósfera*, *25*(1), 1–22.

Sagredo, E. A., & Lowell, T. V. (2012). Climatology of Andean glaciers: A framework to understand glacier response to climate change. *Global and Planetary Change*, *86–87*, 101–109. https://doi.org/10.1016/j.gloplacha.2012.02.010

Santana, R. (1967). Rasgos de la glaciación cuaternaria en "El Manzanar". Valle del Cachapoal. *Andes de Rancagua. Revista Geográfica de Valparaíso*, *1*, 85–98.

Serrano, E., González Trueba, J. J., & Sanjosé, J. J. (2011). Dynamic, evolution and structure of Pyrenean rock glaciers. *Cuadernos de Investigacion Geografica*, *37*(2), 145–170. https://doi.org/10.18172/cig.1260

Wahrhaftig, C., & Cox, A. (1959). Rock glaciers in the Alaska range. *Geological Society of America Bulletin*, *70*(4), 383–436. https://doi.org/10.1130/0016-7606(1959)70[383:RGITAR]2.0.CO;2

Whalley, W. B., & Azizi, F. (2003). Rock glaciers and protalus landforms: Analogous forms and ice sources on Earth and Mars. *Journal of Geophysical Research: Planets*, *108*(4), https://doi.org/10.1029/2002JE001864

Wyrwoll, K.-H. (1977). Causes of rock-slope failure in a cold area: Labrador-Ungava. In D. R. Coates (Ed.), *Landslides* (Vol. 3, pp. 59–67). Geological Society of America. https://doi.org/10.1130/REG3-p57.

Zech, J., Terrizzano, C., García-Morabito, E., Veit, H., & Zech, R. (2017). Timing and extent of late pleistocene glaciation in the arid central Andes of Argentina and Chile (22°-41°S). *Cuadernos de Investigación Geográfica*, *43*(2), 697–718. https://doi.org/10.18172/cig.3235

Zech, R., Kull, C., Kubik, P. W., & Veit, H. (2007). LGM and Late Glacial glacier advances in the Cordillera Real and Cochabamba (Bolivia) deduced from 10 be surface exposure dating. *Climate of the Past*, *3*, 623–635. www.clim-past.net/3/623/2007/.

Zech, R., May, J. H., Kull, C., Ilgner, J., Kubik, P. W., & Veit, H. (2008). Timing of the late quaternary glaciation in the Andes from ~15 to 40° S. *Journal of Quaternary Science*, *23*(6–7), 635–647. doi:10.1002/jqs.1200